HHS Public Access

Author manuscript

Nat Immunol. Author manuscript; available in PMC 2012 December 12.

Published in final edited form as:

Nat Immunol. ; 12(7): 639–646. doi:10.1038/ni.2053.

The development of inducible Bronchus Associated Lymphoid Tissue (iBALT) is dependent on IL-17

Javier Rangel-Moreno[1,*], **Damian M. Carragher**[2,*], **Maria de la Luz Garcia-Hernandez**[1], **Ji Young Hwang**[1], **Kim Kusser**[1], **Louise Hartson**[1], **Jay K. Kolls**[3], **Shabaana A. Khader**[4], and **Troy D. Randall**[1]

[1]Department of Medicine, Division of Allergy Immunology and Rheumatology, University of Rochester Medical Center, Rochester, NY 14642

[2]Trudeau Institute, Saranac Lake, NY 12983

[3]Department of Genetics, Louisiana State University Health Sciences Center, New Orleans, LA 70112

[4]Department of Pediatrics, Division of Infectious Diseases, University of Pittsburgh School of Medicine, Pittsburgh, PA 15224

Abstract

Ectopic or tertiary lymphoid tissues, such as inducible bronchus-associated lymphoid tissue (iBALT), form in non-lymphoid organs after local infection or inflammation. However, the initial events that promote this process remain enigmatic. Here we show that iBALT formed in murine lungs as a consequence of pulmonary inflammation during the neonatal period. Although $CD4^+CD3^-$ lymphoid tissue inducer (LTi) cells were found in neonatal lungs, particularly after inflammation, iBALT was formed in mice lacking LTi cells. Instead, we found that interleukin 17 (IL-17) produced by $CD4^+$ T cells was essential for iBALT formation. IL-17 acted by promoting the lymphotoxin-α-independent expression of CXCL13, which was important for follicle formation. These results suggest that IL-17-producing T cells are critical for the development of ectopic lymphoid tissues.

Introduction

Inducible bronchus associated lymphoid tissue (iBALT) is an ectopic lymphoid tissue that forms in the lungs following pulmonary inflammation or infection[1,2]. Like conventional lymphoid tissues, iBALT has separated B and T cell areas, follicular dendritic cells (FDCs),

Correspondence should be addressed to T.D.R. (Troy_Randall@urmc.rochester.edu), Department of Medicine, Division of Allergy, Immunology and Rheumatology, Box 695, University of Rochester Medical Center, Rochester, NY 14642, Phone 585-276-4613, Fax 585-276-2576.

*These authors contributed equally to the manuscript

Author contribution statement.

J.R-M., D.M.C., M.L.G-H. and T.D.R. designed the experiments. J.R-M., D.M.C., M.LG-H., J.Y.H, K.K. and L.H. performed the experiments. J.R-M and T.D.R. wrote the paper. J.K.K., S.A.K. and T.D.R. edited the paper and provided the funding. The authors declare that they have no competing financial interests.

resident dendritic cells (DCs), high endothelial venules (HEVs) and lymphatics[3]. Once formed, iBALT collects antigen and antigen-bearing DCs from the airways and primes naïve B and T cells[3,4], supports germinal center reactions[3] and generates effector and memory T cells as well as long-lived plasma cells that seed the lung and the bone marrow[5,6]. Memory T and B cells as well as plasma cells are maintained in iBALT and respond locally to secondary challenge[5]. Thus, iBALT promotes rapid and efficient immune responses to pulmonary pathogens.

In humans, iBALT is often associated with chronic diseases, such as rheumatoid arthritis[7], tuberculosis[8] and chronic obstructive pulmonary disease (COPD)[9]. Each of these diseases is associated with persistent exposure to antigen or, in the case of COPD, exposure to cigarette smoke, which causes chronic inflammation and initiates the formation of ectopic lymphoid follicles - a process known as lymphoid neogenesis[2,10,11]. The developmental pathways leading to lymphoid neogenesis have been extensively studied and closely parallel the pre-programmed development of conventional lymph nodes[2,11]. For example, lymph node development is initiated by lymphoid tissue inducer (LTi) cells, which promote the differentiation of mesenchymal cells into stromal cell types that recruit and organize lymphocytes[12]. LTi cells express the chemokine receptors, CXCR5 and CCR7, which promote their homing to sites of future lymph node development[13]. Once there, LTi cells express lymphotoxin (LT)[14], which engages its receptor LTβR on mesenchymal cells and initiates their differentiation and maintains the expression of CXCL13, the ligand for CXCR5, as well as CCL19 and CCL21, the ligands for CCR7 (ref. 15). These same molecules are involved in lymphoid neogenesis, as the transgenic expression of CXCL13 (ref. 16), CCL21 (ref. 17) or LTα[10] in non-lymphoid organs promotes the development of fully functional ectopic lymphoid organs. Moreover, these chemokines and cytokines are highly expressed in ectopic lymphoid tissues that develop in response to infection or inflammation[3,18] and their blockade or genetic deletion disrupts follicle formation[19,20]. Despite the parallels between conventional lymph node development and the formation of ectopic follicles, the initial events and the cell types that begin the process of lymphoid neogenesis remain unknown.

Here we show that the development of murine iBALT following lipopolysaccharide (LPS)-induced inflammation preferentially occurs in neonates during the first week after birth and persists for months in the absence of additional stimulation. Despite this developmental window, the formation of iBALT occurs independently of LTi cells, which require the transcription factors RORγ and Id2, and instead depends on the production of IL-17 by T cells. In turn, IL-17 triggers the LT-independent expression of CXCL13 and CCL19, which recruit and organize lymphocytes. Once established, the architecture of iBALT is maintained by homeostatic expression of CXCL13, CCL19 and LT. Thus, we have defined a new step in the formation of ectopic lymphoid follicles.

Results

iBALT develops following pulmonary inflammation in neonates

We previously found that iBALT formed easily following influenza infection in mice lacking conventional secondary lymphoid organs[3,5,18]. However, a single influenza infection

in adult C57BL/6 mice only elicited disorganized lymphoid clusters consisting primarily of B cells (not shown). Given the link between chronic inflammation and the formation of ectopic follicles, we attempted to establish iBALT by repeatedly administering LPS to the lungs of C57BL/6 mice and then infecting them with influenza, but again we observed disorganized lymphoid clusters rather than discreet areas of iBALT (not shown). Based on previous studies showing that the injection of developing lymph node stroma into the skin of neonatal mice led to the formation of ectopic lymphoid tissues[21], we next intranasally administered LPS to neonatal mice, infected them with influenza when they were 6 weeks old and then examined the lungs by histology 3 weeks later. We found that mice treated in this fashion developed highly organized areas of iBALT containing multiple B cell follicles separated by well-defined T cell areas (Fig. 1a). In contrast, when we performed a similar procedure, but administered LPS to 2-week-old mice (Fig. 1b) or to 3-week-old mice (Fig. 1c), the mice developed disorganized B cell clusters that lacked defined T cell areas or FDC networks. Similar results were observed over a range of LPS doses (1–10 μg) and when we substituted CpG oligonucleotides for LPS (not shown).

To determine whether the combination of LPS and influenza was unique in its ability to trigger iBALT formation, we administered either PBS (Fig. 1d) or LPS (Fig. 1e) to neonatal mice, then administered LPS to both groups when they were 6 weeks old and performed histology 3 weeks later. Again we found that mice treated with LPS as adults did not form organized BALT areas (Fig. 1d), whereas mice treated with LPS as neonates and then again as adults formed well-defined areas of iBALT (Fig. 1e). Thus, pulmonary exposure to inflammatory stimuli during a narrow developmental window in neonatal mice promotes the formation of iBALT.

Role of monocytes and dendritic cells in iBALT formation

Published data show that the maintenance of iBALT is dependent on $CD11c^+$ DCs[4,6]. Given that LPS is a potent inflammatory stimulus, we hypothesized that it would promote the accumulation of DCs and other inflammatory cells in the lung that would facilitate iBALT formation. Consistent with this hypothesis, we found that intranasal administration of LPS to neonates resulted in substantial accumulation of neutrophils, monocytes and $CD11b^{hi}CD103^-$ DCs in the lung (Fig. 2a), but did not change the number of $CD11b^{lo}CD103^+$ DCs (Fig. 2a). To confirm previous data showing that $CD11c^+$ cells were required for iBALT maintenance, we intranasally administered LPS to neonatal CD11c-DTR mice, administered diptheria toxin (DT) one day before the last LPS administration and collected lungs one week later. As expected, we found very few and much smaller iBALT areas in DT-treated mice (not shown). Thus, $CD11c^+$ cells are important for the formation of iBALT in LPS-treated neonates just as they are in influenza-infected adults.

Since monocytes are typically recruited to inflammatory sites via CCR2 (ref. 22) and since some populations of DCs in mucosal lymphoid tissues are dependent on CCR6 (ref. 23), we next tested whether CCR2 or CCR6 were important for iBALT formation. However, we found that iBALT developed normally in both *Ccr2*$^{-/-}$ and *Ccr6*$^{-/-}$ mice (Fig. 2b). In addition, the total area of the lymphoid follicles in *Ccr2*$^{-/-}$ and *Ccr6*$^{-/-}$ mice was indistinguishable from that in wild-type C57BL/6 mice (Fig. 2c). Finally, we observed that

CXCL13 and CCL19, chemokines important for the organization of lymphoid tissues[15], were induced to the same extent in C57BL/6, *Ccr2*$^{-/-}$ and *Ccr6*$^{-/-}$ mice (Fig. 2d). Thus, despite the dependence of iBALT on DCs, neither CCR2 nor CCR6 are required for the normal development of iBALT.

iBALT forms independently of LTi cells

The development of conventional secondary lymphoid organs is dependent on the activity of CD4^{+}CD3^{-} LTi cells[24,25]. Given that LTi cells are more prevalent in neonatal mice than in adults, we hypothesized that neonatal exposure to LPS would recruit LTi cells to the lung where they would trigger iBALT development. To test this hypothesis, we initially enumerated CD4^{+} lineage-negative (Lin^{-}) cells in the lungs of PBS-treated and LPS-treated neonatal mice. We found that CD4^{+}Lin^{-} cells were present in the lungs of both groups, but that the frequency of these cells was about 4-fold higher in the LPS-treated group (Fig. 3a). In addition, the number of CD4^{+}Lin^{-} cells was about 3-fold higher in LPS-treated lungs and the number of CD4^{+}CXCR5^{+}Lin^{-} cells was 4-fold higher in LPS-treated lungs (Fig. 3b).

To assess whether LTi cells were required for the formation of iBALT, we administered LPS to neonatal *Rorc*$^{-/-}$ mice and *Id2*$^{-/-}$ mice, both of which fail to develop LTi cells and consequently lack lymph nodes[26,27]. We also administered LPS to neonatal *Lta*$^{-/-}$ mice and to neonatal mice lacking the chemokines CXCL13, CCL19 and CCL21a (DKO mice), both of which fail to develop lymph nodes due to poor mesenchymal cell differentiation and poor LTi homing[28,29]. We found that both *Rorc*$^{-/-}$ and *Id2*$^{-/-}$ mice developed normal iBALT areas (Fig. 3c), but although B and T cells accumulated in *Lta*$^{-/-}$ mice, they were not separated into distinct areas, FDCs did not form and PNAd-expressing HEVs were undetectable (Fig. 3c). Similar results were observed using sLTβR to block the engagement of the LTβR (not shown). Finally, the chemokine-deficient DKO mice accumulated B and T cells in their lungs, but they failed to form distinct zones and FDCs were not apparent. However, DKO mice did form PNAd-expressing HEVs (Fig. 3c). Thus, it seems that the formation and organization of iBALT does not require RORγ-dependent or Id2-dependent LTi cells, but does require LTα and homeostatic chemokines for lymphoid organization.

IL-17 contributes to iBALT formation

Since LTi cells were not required for the formation of iBALT, it was not immediately apparent why iBALT developed preferentially in neonatal mice. Therefore, we next examined the expression of a variety of candidate genes that might be differentially expressed in neonatal and adult mice following pulmonary exposure to LPS. We found that LTβ and LIGHT, both ligands for the LTβR, were induced following LPS exposure, but were induced at similar or higher abundance in weanlings and adult mice relative to neonates (Fig. 4). The expression of CCL19 was also similarly induced in neonates, weanlings and adults. However, LPS induced more CXCL13 expression in neonates compared to either weanlings or adults and the expression of the p19 subunit of IL-23 and IL-17A were induced to much higher amounts in neonates and weanlings compared to adults (Fig. 4). Since IL-23 is important for the stability of IL-17-producing T cells[30], these results suggested that IL-17-producing T cells may preferentially accumulate in the lungs of neonatal mice and may promote the formation of iBALT.

To test whether IL-17 played a role in iBALT development, we administered LPS to various gene-deficient mice (Fig. 5a–e). We found that although iBALT areas were present in the lungs of *Il17ra*$^{-/-}$ mice (Fig. 5b), these structures were smaller and less numerous than those in C57BL/6 mice. In contrast, we found iBALT areas of normal size and composition, but fewer in number, in LPS-treated *Il23p19*$^{-/-}$ mice (Fig. 5c). We also found that iBALT formation was impaired in *Il17a*$^{-/-}$ mice (Fig. 5d). Finally, even though the numbers and size of iBALT areas were reduced in *Il17ra*$^{-/-}$ and *Il17a*$^{-/-}$ mice, the architecture of the remaining iBALT areas was not as disrupted as in *Lta*$^{-/-}$ mice (Fig. 5e). To get a more quantitative assessment of iBALT in the various strains of mice, we performed a morphometric analysis and determined the number and size of lymphoid areas, B cell follicles and FDC networks observed by histology and calculated the total area of iBALT in a typical section (Fig. 5f). Together, these data support the conclusion that IL-17A and, to a lesser extent, IL-23 are important for the formation of iBALT.

Given that IL-17 signaling promotes the expression of CXCL9, CXCL10 and CXCL11, which in turn recruit inflammatory cells, we hypothesized that IL-17 may also trigger the expression of CXCL13, CCL19, and CCL21 - all of which are involved in the initial formation of conventional lymphoid organs and help to maintain their structure[28]. We found that the expression of both CXCL13 and CCL19, but not CCL21, was induced in the lungs of LPS-treated C57BL/6 mice, but the expression of these chemokines was not induced to the same extent in *Il17ra*$^{-/-}$ mice (Fig. 5g). In contrast, LPS induced normal expression of both CXCL13 and CCL19 in *Il23p19*$^{-/-}$ and *Lta*$^{-/-}$ mice (Fig. 5g). As a control, we also examined the expression of CXCL9, CXCL10 and CXCL11, chemokines known to be induced in response to IL-17. As expected, we found that LPS substantially increased the expression of these chemokines and that the loss of IL-17RA reduced their expression (Fig. 5h). In contrast, the expression of CXCL9, CXCL10 and CXCL11 was not impaired in *Il23p19*$^{-/-}$ mice (Fig. 5h). Finally, the expression of CXCL10 and CXCL11 was partially reduced in *Lta*$^{-/-}$ mice, although not to the extent seen in *Il17ra*$^{-/-}$ mice (Fig. 5h).

To confirm using an independent method that IL-17 could promote the expression of CXCL13 and CCL19, we isolated pulmonary fibroblasts from neonatal mice, cultured them for 6 h with recombinant IL-17A or tumor necrosis factor (TNF) and analyzed the expression of homeostatic chemokines by quantitative PCR. Consistent with the results from whole lungs, we found that treatment with IL-17A or TNF promoted increased expression of both CXCL13 and CCL19, but not CCL21 (Fig. 5i). However, combined treatment with both IL-17A and TNF did not increase the expression of either CXCL13 or CCL19 above that seen with either cytokine alone (not shown).

IL-17A is required to initiate, but not to maintain iBALT

To determine the kinetics of iBALT formation and observe how long it lasted, we intranasally administered LPS to neonatal mice and performed histology at the indicated times after the last LPS administration. We observed rudimentary iBALT structures within 6 h of the last LPS administration consisting of small clusters of B and T cells with nascent FDC networks (Fig. 6a). However, within 1 week after the final LPS administration we observed well-developed B cell follicles that were maintained for at least 10 weeks in the

absence of additional stimulation (Fig. 6a). Following pulmonary infection with influenza, the iBALT areas enlarged (Fig. 6a) and in many cases developed germinal centers (not shown), consistent with our previous observations[3]. We also quantified the size of FDC networks in iBALT at the different times following LPS administration and found that FDCs rapidly expanded following cessation of LPS administration and then gradually declined over time in the absence of new stimulation. However, FDC networks expanded again following influenza infection (Fig. 6b). Thus, iBALT formed rapidly following acute inflammation and, once formed, persisted in the lung for at least several months.

To determine at what steps IL-17 and LT were important in iBALT formation, we intranasally administered LPS to neonatal mice and treated them with either soluble LTβR (sLTβR) or anti-IL-17A before the last LPS treatment (prior to iBALT formation) or 1 week after the last LPS administration (when iBALT is already formed) and enumerated iBALT areas in the lung 1 week later. We found that treatment with sLTβR and anti-IL-17 reduced the number of B cell clusters and FDC networks when given before iBALT formation, but not when given after iBALT formation (Fig. 6c, top). In contrast, the sizes of the B cell clusters and FDC networks were reduced by LTβR blockade both before and after iBALT formation, whereas the size of B cell clusters was only reduced by anti-IL-17 when it was given prior to iBALT formation (Fig. 6c, middle). Overall, we found that LTβR blockade reduced the total areas of B cell clusters and FDC networks when give either before or after iBALT formation, whereas IL-17A blockade only affected the total areas of B cell clusters and FDC networks when given before iBALT formation (Fig. 6c, bottom). Thus, we conclude that IL-17 signaling is involved during the initiation of iBALT formation, but not in the maintenance of iBALT, whereas LT signaling seems to be involved in both early and late steps.

IL-17-producing T cells contribute to iBALT formation

To determine what cells produced IL-17 in the lungs of LPS treated mice, we purified naïve $CD4^+$ T cells from adult spleen and purified non-T cells, αβT cells, γδT cells and total $CD4^+$ cells from the lungs of LPS-treated neonates and assayed IL-17A expression by quantitative PCR. We found that naïve $CD4^+$ cells as well as non-T cells from the lungs of LPS-treated mice expressed little IL-17 (Fig. 7a), whereas αβT cells, γδT cells and $CD4^+$ cells from the lungs of LPS-treated mice abundantly expressed IL-17 (Fig. 7a). To determine whether IL-17-expressing cells had any physical proximity to iBALT, we probed sections of LPS-treated neonatal lungs with antibodies to IL-17A. We found that essentially all of IL-17A-producing cells found in developing iBALT areas co-expressed CD4 (Fig. 7b). Given that both αβ and γδT cells expressed IL-17 and that many of the γδT cells in the lung also expressed CD4 (not shown), we also determined the presence of these two cell types in iBALT areas. We found that $CD3^+$ T cells (red) were located surrounding the B cell follicle in iBALT (Fig. 7c) and that $CD3^+$ γδT cells (violet) were located in a similar area (Fig. 7d). Moreover, the $CD3^+$ γδT cells accounted for about a third of the T cells present in iBALT, suggesting that αβT cells (both $CD4^+$ and $CD8^+$) accounted for the remainder. Thus, both αβT cells and γδT cells are present in iBALT and are likely to contribute to IL-17 production.

To directly determine the contribution of T cells to the formation of iBALT, we next administered LPS to neonatal T cell-deficient (*Tcrbd*$^{-/-}$) mice. We found that LPS-treated *Tcrbd*$^{-/-}$ mice formed fewer and smaller B cell clusters that completely lacked FDC networks (Fig. 7a). However, when we adoptively transferred CD4^{+} T cells from LNs of LPS-treated mice to neonatal mice prior to the administration of LPS, we again observed the normal formation of iBALT (Fig. 7e). Since *Tcrbd*$^{-/-}$ mice could still have LTi cells that might contribute to the formation of iBALT, we next administered LPS to neonatal *Rorc*$^{-/-}$ mice that had either been depleted (or not) of CD4^{+} T cells. We found well-developed iBALT areas in *Rorc*$^{-/-}$ mice, but only a few small clusters of B cells in CD4-depleted *Rorc*$^{-/-}$ mice (Fig. 7f). As a control, we showed that the antibody depletion eliminated both CD4^{+} αβT cells and CD4^{+} γδT cells (Fig. 7g). Thus, iBALT development is dependent on CD4^{+} T cells.

To determine whether αβT cells or γδT cells preferentially contributed to iBALT formation, we purified γδT cells and αβT cells from LPS-treated neonatal mice and adoptively transferred these populations to LPS-treated neonatal *Tcrbd*$^{-/-}$ mice. We found that γδT cells facilitated the development of iBALT, but that αβT cells generated larger areas of iBALT and that the transfer of both subsets provided an additive effect (Fig. 7h). Given that conventional αβT cells could efficiently generate iBALT, we next determined whether IL-17-producing T_H17 cells could induce iBALT. To test this possibility, we activated OVA-specific OT-II cells *in vitro* under conditions that would generate CXCR5-expressing T follicular helper (T_{FH}) cells, IL-17-producing T_H17 cells, or a combination of conditions that would generate CXCR5-expressing, IL-17-producing T_{FH} ($T_{FH}17$) cells (Fig. 7i). These cells were then transferred to neonatal *Tcrbd*$^{-/-}$ mice, which were then treated with LPS and OVA. Although we could find occasional areas of iBALT in mice that received T_{FH} cells (Fig. 7i), we found larger and more numerous areas of iBALT in mice that received T_H17 cells and many more (and larger) areas in mice that received $T_{FH}17$ cells (Fig. 7j). As controls, we also transferred T_H1 and T_H2 cells, which were the weakest inducers of iBALT formation (not shown). Thus, CXCR5-expressing, IL-17-producing $T_{FH}17$ cells efficiently trigger the formation of ectopic follicles in the lung.

Discussion

Here we show that IL-17-producing T cells are involved in the formation of ectopic lymphoid follicles in the lung, and that IL-17 appears to act by triggering the expression of CXCL13 and CCL19 independently of LT signaling. Thus, we propose a new model of ectopic follicle formation in which the initial step is the production of IL-17 by non-LTi cells, such as T cells. In turn, IL-17 promotes the expression of CXCL13 and CCL19, which recruits B and T cells and maintains the structure of FDC networks. Once the initial inflammatory response resolves, the expression of CXCL13 and CCL19 as well as the overall architecture of iBALT is maintained by the homeostatic interaction of LT-expressing lymphocytes with LTβR-expressing stromal cells or vascular endothelial cells. This model is also consistent with the requirement of T cells, but not LTi cells, for the formation of ectopic follicles in transgenic mice expressing CCL21 in the thyroid[31]. Moreover, these data suggest that simultaneously targeting both IL-17 and LT signaling pathways may be beneficial in

diseases such as Sjogren's syndrome or multiple sclerosis, in which the development of ectopic follicles is linked to local pathology.

A striking observation from these studies is that iBALT forms much more easily in neonates than in adults, a fact that we initially attributed to the higher frequency of LTi cells in neonates. However, our results with *Rorc*$^{-/-}$ and *Id2*$^{-/-}$ mice suggest that LTi cells are not required for the development of iBALT - a scenario similar to the RORγ- and Id2-independent development of tear duct-associated lymphoid tissue (TALT)[32] and the milky spots of the omentum[33] as well as the RORγ-independent (but Id2-dependent) development of nasal-associated lymphoid tissue (NALT)[34,35]. All of these tissues develop in the neonatal period and may be dependent on different types of LTi cells or perhaps IL-17-producing T cells. A caveat to this explanation is that, in addition to the development of LTi cells, RORγ is important for the production of IL-17 by T cells - both αβT cells[36] as well as γδT cells (not shown). Thus, the formation of ectopic lymphoid tissues in *Rorc*$^{-/-}$ mice may rely on compensatory mechanisms as suggested by studies looking at the development of ectopic follicles in the colons of *Rorc*$^{-/-}$ mice[37]. Alternatively, despite reduced IL-17 production by *Rorc*$^{-/-}$ T cells, the residual IL-17 produced by T cells may trigger low expression of CXCL13 in the lung, which in mice lacking conventional secondary lymphoid organs, may be sufficient to recruit lymphocytes and initiate lymphoid organogenesis.

Assuming that iBALT formation is not dependent on LTi cells, but is instead dependent on IL-17-producing T cells, a different hypothesis is required to explain the preferential development of iBALT in neonates. For example, γδT cells first emerge from fetal progenitors prior to αβT cells[38], suggesting they are the first T cells available during the neonatal period. γδT cells also express IL-17 in response to microbial products[39] and many γδT cells are located in the lung, where they would be positioned to promote iBALT development. Moreover, Tregs are not exported to the periphery during the first week after birth and as a result, neonatal thymectomy leads to autoimmunity[40]. Given that the lack of proper Treg homing in CCR7-deficient mice appears to promote spontaneous iBALT formation[41], it is possible that the relative paucity of Tregs and relative abundance of IL-17-producing γδT cells in neonates may ease the formation of iBALT following pulmonary inflammation. The preferential formation of iBALT in neonates is also consistent with observations in humans showing that iBALT is infrequently found in healthy adults[42,43], but is more frequently found in the lungs of healthy children [44]. Moreover, the incidence of iBALT approaches 100% in the lungs of neonates with pulmonary infections[45].

Of course, the formation of iBALT is not exclusively restricted to the neonatal period, as iBALT can be observed in adult mice following pulmonary viral[4,6] and bacterial infections[46,47] as well as the pulmonary administration of cigarette smoke[48], particulates or protein nanoparticles[49]. It is also observed in patients with a variety of inflammatory conditions, such as COPD[9], and rheumatoid arthritis[7]. Although these conditions often develop in adults, it is unknown whether the patients with iBALT experienced pulmonary inflammation as neonates, which may have conditioned their lungs to form iBALT as adults. Nevertheless, we would suggest that conditions that lead to the recruitment and activation of any IL-17-producing cell type, including γδT cells, Th17 cells, NK cells and LTi cells, is

likely to lead to the development of ectopic structures, particularly if the stimulus is chronic, such as in rheumatoid arthritis[50] and multiple sclerosis[51] or upon chronic infection.

Given the association of Th17 cells with bacterial infections[52], it is not surprising that the frequency of Th17 cells in a particular individual is dependent on their history of exposure to pathogens and even commensal bacteria in the gut. Similar observations have been made in mice. In particular, those mice exposed to Segmented Filamentous Bacteria (SFB) in the gut have high frequencies of Th17 cells[53]. Since mice from different commercial vendors and institutional colonies have widely different gut flora, including SFB, each colony has different frequencies of Th17 cells, which leads to different biological outcomes in terms of inflammatory diseases, including autoimmunity[54]. The mice used in our study were imported to the Trudeau Institute, where they were rederived by embryo transfer into germ-free foster mothers that were reconstituted with altered Schaedler's flora, a mix of eight species that does not include SFB[55]. These animals were then maintained in a barrier facility at Trudeau Institute and then imported to a barrier facility at the University of Rochester. Therefore, we suspect that the limited diversity of gut flora in our mice is one reason that we do not observe the development of iBALT as adults when exposed to influenza infection or intranasally administered LPS. In contrast, other investigators using genetically identical mice are likely to obtain different results depending of the gut flora in their colonies.

In summary, our results establish a new paradigm of how ectopic lymphoid follicles form in non-lymphoid tissues and show that the initial step in ectopic follicle formation is dependent on IL-17, which triggers the maturation of the FDC network and promotes the expression of CXCL13 and CCL19 independently of LT. In turn, these chemokines recruit lymphocytes, which form organized B and T cell domains that are maintained via LT-dependent homeostatic mechanisms once inflammation is resolved.

Methods

Mice and intranasal administrations

C57BL/6, B6.129S2-Lta^{tm1Dch}/J (*Lta*$^{-/-}$), B6.129P2-Tcrb^{tm1Mom}Tcrd^{tm1Mom}/J (*Tcrbd*$^{-/-}$), B6.FVB-Tg(Itgax-DTR/EGFP)57Lan/J (CD11c-DTR) and B6.129S4-Ccr2^{tm1Ifc}/J (*Ccr2*$^{-/-}$) mice were obtained from Jackson Labs. *Ccr6*$^{-/-}$ mice were obtained from S. Lira (Mt. Sinai School of Medicine). *Rorc*$^{-/-}$ and *Id2*$^{-/-}$ mice were obtained from D. Littman (NYU). *Cxcl13*$^{-/-}$ and *plt/plt* mice were obtained from J. Cyster (UCSF) and crossed to generate mice lacking CXCL13, CCL19 and CCL21a (DKO mice). These strains were imported to Trudeau Institute and rederived. Rederived mice were then imported to a barrier facility at the University of Rochester, where they were bred and maintained. Rederived OT-II mice were obtained from L. Haynes (Trudeau Institute). *Il17ra*$^{-/-}$ and *Il17a*$^{-/-}$ mice were obtained from investigator-owned colonies that had been rederived at Taconic laboratories.

Litters of neonatal or adult mice were anesthetized with isofluorane and intranasally administered 1–10 μg LPS in 10 μl (0–2 week-old mice) or in 30 μl (2-week and older mice) every other day over 10 days (5 administrations). Anti-IL-17A (R&D Systems) and sLTβR (J. Browning - Biogen Idec) were administered at 25 μg/mouse and 50 μg/mouse respectively on the days indicated. In some cases, mice were intranasally infected with 500

egg infectious units of influenza A/PR/8/34 in 50 μl. All procedures were approved by the Trudeau Institute IACUC and the University of Rochester UCAR and were performed according to the standards outlines by the National Research Council.

Generation of T_H cells and adoptive transfers

$CD4^+$ T cells were purified from spleens of OT-II mice using anti-CD4 beads (Miltenyi Biotec). T_{FH} cells were generated by co-culturing purified OT-II cells for 4 d with mitomycin C-treated, LPS-activated B cells in media containing 10 μg/ml OVA peptide, 20 μg/ml anti-TGF-β (1D11), 10 μg/ml anti-IL-4 (11B11), 10 μg/ml anti-IFN-γ (XMG1.2) and 50 ng/ml IL-21. T_H17 cells were generated by culturing purified OT-II cells with mitomycin C-treated, LPS-activated B cells in media containing 10 μg/ml OVA peptide (New England Peptide), 10 μg/ml anti-IFN-γ, 10 μg/ml anti-IL-4, 10 ng/ml TNF, 0.5 ng/ml TGFβ,10 ng/ml IL-1β, 20 ng/ml IL-6 (Peprotech), 50 ng/ml IL-21 and 25 ng/ml IL-23 (R&D Systems). $T_{FH}17$ cells were generated by first culturing OT-II cells under T_{FH} conditions for 4 d and then switching the cells to T_H17 conditions for 4 additional days.

Histology and immunofluorescence

Lungs from LPS-treated mice were perfused with a 50:50 mixture of OCT (Sakura Finetek) in PBS and frozen over liquid nitrogen. Frozen sections were cut at 5 μm, fixed in cold acetone for 10 min, left to dry at 25 °C and stored at −70 °C until use. For histological analysis, lung sections were stained with Diff Quick. For immunofluorescent analysis, slides were hydrated in PBS and blocked for 30 min at 25 °C with 10 μg/ml of Fc Block and 5% normal donkey serum in PBS. After blocking, cocktails of primary antibodies in PBS, including goat anti-CD3ε (Santa Cruz Biotechnology), CD11c (HL3), B220 (RA3-6B2) and γδTCR (GL3) all from BD Biosciences, CD21/CD35 (7E9), NKp46 (29A1.4) anti-IL-17 (TC11-18H10.1) all from Biolegend and peanut agglutinin (PNA) from Sigma were incubated on the slides for 30 min at 25 °C. Primary antibodies were detected with donkey anti-goat-Alexa fluor-568, rabbit anti-FITC-Alexa fluor-488, streptavidin-Alexa fluor-555 (Invitrogen Life Sciences) or streptavidin-APC (BD Biosciences). Slides were mounted with Slow Fade Gold Antifade with DAPI (Molecular probes, Invitrogen Life Sciences). Images were collected with a Zeiss Axioplan 2 microscope and recorded with a Zeiss Axiocam digital camera (Zeiss). Images recorded in the far-red channel were pseudocolored blue. Morphometric analysis was performed using the Outline tool in the Zeiss Axiovision software.

Flow cytometry

Lungs were perfused with 10 mM EDTA in HBSS and were chopped with a single edge blade. Tissue fragments were digested in media containing 0.6 mg/ml collagenase A and 30 μg/ml DNAse I (both from SIGMA) for 30 at 37 °C minutes in a shaker and then mechanically disrupted by pushing through a metal strainer. Red cells were lysed and single cell suspensions were incubated with 1 μg/ml Fc block for 30 min on ice. Cocktails of antibodies (anti-CD127 (B12-1), CD8 (53.6.7), CD11b (M1/70), CD11c (HL3), B220 (RA3-6B2), CXCR5 (2G8) and γδTCR (GL3) from BD Biosciences and anti-CD19 (MB19.1), NK1.1 (NKR-P1C), CD3e (17A2) and CD4 (GK1.5) from eBisocience) were

added and incubated at 4 °C for 15 min. Finally, cells were washed and re-suspended with propidium iodide.

RNA extraction and PCR

Total RNA was isolated from lungs using TRIzol (Invitrogen) according to the manufacturer's specifications and re-purified using RNeasy mini kit (QIAGEN). 2.5 μg of RNA were reverse transcribed with Superscript II and random primers (Invitrogen) and cDNA was resuspended at 10 μg/μl. 50 ng of cDNA were amplified with specific primers and probes from Applied Biosystems, using Taqman Universal PCR master mix and following the manufacturer's protocol. The expression of individual mRNAs was calculated by subtracting the CT of GAPDH from the CT of the test mRNA and then taking the inverse log(2) of the difference.

Purification of αβT cells and γδT cells

Lungs and draining LNs were obtained 1 week after the last LPS administration and non-T cells were obtained by positive selection for cells that expressed CD11b, CD11c, CD19, B220, NK1.1 and Gr-1 using MACS beads (Miltenyi Biotec). The flow-through cells were subjected to positive selection to purify γδT cells and the remaining flow-through cells were again subjected to positive selection for Thy-1 to purify αβT cells. In separate procedures, naïve $CD4^+$ cells were purified from the spleens of naïve adult mice and $CD4^+$ cells were also purified from the lungs of LPS-treated mice using MACS (Miltenyi Biotec).

Isolation and culture of primary pulmonary fibroblasts

Lungs from 10 day-old mice were digested with collagenase A and DNAase and single cell suspensions were cultured in 6-well plates. Non-non-adherent cells were removed after 2 days and fresh media was added to the remaining cells, which were grown for 3 more days and then expanded in fresh 6-well plates. When they reached 70% confluence, they were treated with either 200 ng/ml IL-17A or 60 ng/ml TNF (Peprotech) for 6 h. RNA was extracted, cDNA was prepared and quantitative PCR was performed to determine changes in mRNA expression in treated cells, compared with non-treated fibroblasts.

Statistical analysis

Data was analyzed using a two-tailed Student’s t test.

Acknowledgements

The authors would like to thank L. LaMere and A. Boucher for animal husbandry as well as S. Lira (Mt. Sinai School of Medicine), D. Littman (NYU) and J. Cyster (UCSF) for providing various mouse strains and J. Browning (Biogen Idec) for providing the sLTβR. This work was supported by the University of Rochester and by NIH grants HL069409, AI072689 and AI061511 to T.D.R. as well as by the Children's Hospital of Pittsburgh and by NIH grant HL105427 to S.A.K.

References

1. Randall T. Bronchus-Associated Lymphoid Tissue: structure and function. Adv Immunol. 2010
2. Carragher DM, Rangel-Moreno J, Randall TD. Ectopic lymphoid tissues and local immunity. Semin Immunol. 2007; 20

3. Moyron-Quiroz JE, et al. Role of inducible bronchus associated lymphoid tissue (iBALT) in respiratory immunity. Nat Med. 2004; 10:927–934. [PubMed: 15311275]
4. Halle S, et al. Induced bronchus-associated lymphoid tissue serves as a general priming site for T cells and is maintained by dendritic cells. J Exp Med. 2009; 206:2593–2601. [PubMed: 19917776]
5. Moyron-Quiroz JE, et al. Persistence and responsiveness of immunologic memory in the absence of secondary lymphoid organs. Immunity. 2006; 25:643–654. [PubMed: 17045819]
6. GeurtsvanKessel CH, et al. Dendritic cells are crucial for maintenance of tertiary lymphoid structures in the lung of influenza virus-infected mice. J Exp Med. 2009; 206:2339–2349. [PubMed: 19808255]
7. Rangel-Moreno J, et al. Inducible bronchus-associated lymphoid tissue (iBALT) in patients with pulmonary complications of rheumatoid arthritis. J Clin Invest. 2006; 116:3183–3194. [PubMed: 17143328]
8. Ulrichs T, et al. Human tuberculous granulomas induce peripheral lymphoid follicle-like structures to orchestrate local host defence in the lung. J Pathol. 2004; 204:217–228. [PubMed: 15376257]
9. Hogg JC, et al. The nature of small-airway obstruction in chronic obstructive pulmonary disease. N Engl J Med. 2004; 350:2645–2653. [PubMed: 15215480]
10. Kratz A, Campos-Neto A, Hanson MS, Ruddle NH. Chronic inflammation caused by lymphotoxin is lymphoid neogenesis. J Exp Med. 1996; 183:1461–1472. [PubMed: 8666904]
11. Randall TD, Carragher DM, Rangel-Moreno J. Development of secondary lymphoid organs. Ann Rev Immunol. 2008; 26
12. Cupedo T, Kraal G, Mebius RE. The role of CD45+CD4+CD3- cells in lymphoid organ development. Immunol Rev. 2002; 189:41–50. [PubMed: 12445264]
13. van de Pavert SA, et al. Chemokine CXCL13 is essential for lymph node initiation and is induced by retinoic acid and neuronal stimulation. Nat Immunol. 2009; 10:1193–1199. [PubMed: 19783990]
14. Mebius RE, Rennert P, Weissman IL. Developing lymph nodes collect CD4+CD3-LTb+ cells that can differentiate to APC, NK cells, and follicular cells, but notT or B cells. Immunity. 1997; 7:493–504. [PubMed: 9354470]
15. Ngo VN, et al. Lymphotoxin a/b and tumor necrosis factor are required for stromal cell expression of homing chemokines in B and T cell areas of the spleen. J. Exp. Med. 1999; 189:403–412. [PubMed: 9892622]
16. Luther SA, Lopez T, Bai W, Hanahan D, Cyster JG. BLC Expression in Pancreatic Islets Causes B Cell Recruitment and Lymphotoxin-Dependent Lymphoid Neogenesis. Immunity. 2000; 12:471–481. [PubMed: 10843380]
17. Chen SC, et al. Ectopic expression of the murine chemokines CCL21a and CCL21b induces the formation of lymph node-like structures in pancreas, but not skin, of transgenic mice. J Immunol. 2002; 168:1001–1008. [PubMed: 11801632]
18. Rangel-Moreno J, Moyron-Quiroz JE, Hartson L, Kusser K, Randall TD. Pulmonary expression of CXC chemokine ligand 13, CC chemokine ligand 19, and CC chemokine ligand 21 is essential for local immunity to influenza. Proc Natl Acad Sci U S A. 2007; 104:10577–10582. [PubMed: 17563386]
19. Gatumu MK, et al. Blockade of lymphotoxin-beta receptor signaling reduces aspects of Sjogren's syndrome in salivary glands of non-obese diabetic mice. Arthritis Res Ther. 2009; 11:R24. [PubMed: 19222863]
20. Furtado GC, et al. Lymphotoxin beta receptor signaling is required for inflammatory lymphangiogenesis in the thyroid. Proc Natl Acad Sci U S A. 104; 2007:5026–5031.
21. Cupedo T, Jansen W, Kraal G, Mebius RE. Induction of secondary and tertiary lymphoid structures in the skin. Immunity. 2004; 21:655–667. [PubMed: 15539152]
22. Serbina NV, Pamer EG. Monocyte emigration from bone marrow during bacterial infection requires signals mediated by chemokine receptor CCR2. Nat Immunol. 2006; 7:311–317. [PubMed: 16462739]
23. Iwasaki A, Kelsall BL. Localization of Distinct Peyer'ls Patch Dendritic Cell Subsets and Their recruitment by chemokines Macrophage Inflammatory Protein (MIP)3a, MIP-3b, and Secondary Lymphoid Organ Chemokine. J. Exp. Med. 2000; 191:1381–1393. [PubMed: 10770804]

24. Mebius RE, et al. The fetal liver counterpart of adult common lymphoid progenitors gives rise to all lymphoid lineages, CD45+CD4+CD3- cells, as well as macrophages. J Immunol. 2001; 166:6593–6601. [PubMed: 11359812]
25. Cupedo T, Mebius RE. Cellular interactions in lymph node development. J Immunol. 2005; 174:21–25. [PubMed: 15611222]
26. Sun Z, et al. Requirement for RORg in Thymocyte Survival and Lymphoid Organ Development. Science. 2000; 288:2369–2373. [PubMed: 10875923]
27. Yokota Y, et al. Development of peripheral lymphoid organs and natual killer cells depends on the helix-loop-helix inhibitor Id2. Nature. 1999; 397:702–706. [PubMed: 10067894]
28. Luther SA, Ansel KM, Cyster JG. Overlapping roles of CXCL13, interleukin 7 receptor alpha, and CCR7 ligands in lymph node development. J Exp Med. 2003; 197:1191–1198. [PubMed: 12732660]
29. de Togni P, et al. Abnormal development of peripheral lymphoid organs in mice deficient in lymphotoxin. Science. 1994; 264:703–707. [PubMed: 8171322]
30. Zhou L, et al. IL-6 programs T(H)-17 cell differentiation by promoting sequential engagement of the IL-21 and IL-23 pathways. Nat Immunol. 2007; 8:967–974. [PubMed: 17581537]
31. Marinkovic T, et al. Interaction of mature CD3+CD4+ T cells with dendritic cells triggers the development of tertiary lymphoid structures in the thyroid. J Clin Invest. 2006; 116:2622–2632. [PubMed: 16998590]
32. Nagatake T, et al. Id2-, RORgammat-, and LTbetaR-independent initiation of lymphoid organogenesis in ocular immunity. J Exp Med. 2009; 206:2351–2364. [PubMed: 19822644]
33. Rangel-Moreno J, et al. Omental milky spots develop in the absence of lymphoid tissue-inducer cells and support B and T cell responses to peritoneal antigens. Immunity. 2009; 30:731–743. [PubMed: 19427241]
34. Harmsen A, et al. Organogenesis of Nasal Associated Lymphoid Tissue (NALT) occurs independently of lymphotoxin-α (LTα) and retinoic acid receptor-related orphan receptor-γ, but the organization of NALT is LTα-dependent. J. Immunol. 2002; 168:986–990. [PubMed: 11801629]
35. Fukuyama S, et al. Initiation of NALT organogenesis is independent of the IL-7R, LTbetaR, and NIK signaling pathways but requires the Id2 gene and CD3(−)CD4(+)CD45(+) cells. Immunity. 2002; 17:31–40. [PubMed: 12150889]
36. Yang XO, et al. T helper 17 lineage differentiation is programmed by orphan nuclear receptors ROR alpha and ROR gamma. Immunity. 2008; 28:29–39. [PubMed: 18164222]
37. Lochner M, et al. Microbiota-induced tertiary lymphoid tissues aggravate inflammatory disease in the absence of RORgamma t and LTi cells. J Exp Med. 208:125–134. [PubMed: 21173107]
38. Ikuta K, et al. A developmental switch in thymic lymphocyte maturation potential occurs at the level of hematopoietic stem cells. Cell. 1990; 62:863–874. [PubMed: 1975515]
39. Martin B, Hirota K, Cua DJ, Stockinger B, Veldhoen M. Interleukin-17-producing gammadelta T cells selectively expand in response to pathogen products and environmental signals. Immunity. 2009; 31:321–330. [PubMed: 19682928]
40. Bagavant H, Thompson C, Ohno K, Setiady Y, Tung KS. Differential effect of neonatal thymectomy on systemic and organ-specific autoimmune disease. Int Immunol. 2002; 14:1397–1406. [PubMed: 12456587]
41. Kocks JR, Davalos-Misslitz AC, Hintzen G, Ohl L, Forster R. Regulatory T cells interfere with the development of bronchus-associated lymphoid tissue. J Exp Med. 2007; 204:723–734. [PubMed: 17371929]
42. Tshering T, Pabst R. Bronchus associated lymphoid tissue (BALT) is not present in normal adult lung but in different diseases. Pathobiol. 2000; 68:1–8.
43. Sue-Chu M, et al. Lymphoid aggregates in endobronchial biopsies from young elite cross-country skiers. Am J Respir Crit Care Med. 1998; 158:597–601. [PubMed: 9700140]
44. Heier I, et al. Bronchial response pattern of antigen presenting cells and regulatory T cells in children less than 2 years of age. Thorax. 2008; 63:703–709. [PubMed: 18250182]
45. Ersch J, Tschernig T, Stallmach T. Frequency and potential cause of bronchus-associated lymphoid tissue in fetal lungs. Pediatr Allergy Immunol. 2005; 16:295–298. [PubMed: 15943591]

46. Kahnert A, et al. Mycobacterium tuberculosis triggers formation of lymphoid structure in murine lungs. J Infect Dis. 2007; 195:46–54. [PubMed: 17152008]
47. Chiavolini D, et al. Bronchus-associated lymphoid tissue (BALT) and survival in a vaccine mouse model of tularemia. PLoS One. 5 e11156.
48. Escolar Castellon JD, Escolar Castellon A, Roche Roche PA, Minana Amada C. Bronchial-associated lymphoid tissue (BALT) response to airway challenge with cigarette smoke, bovine antigen and anti-pulmonary serum. Histol Histopathol. 1992; 7:321–328. [PubMed: 1504450]
49. Wiley JA, et al. Inducible Bronchus-associated lymphoid tissue elicited by a protein cage nanoparticle enhances protection in mice against diverse respiratory viruses. PLoS One. 2009; 4 e7142.
50. van den Berg WB, Miossec P. IL-17 as a future therapeutic target for rheumatoid arthritis. Nat Rev Rheumatol. 2009; 5:549–553. [PubMed: 19798029]
51. Segal BM. Th17 cells in autoimmune demyelinating disease. Semin Immunopathol. 32:71–77. [PubMed: 20195867]
52. Khader SA, Gaffen SL, Kolls JK. Th17 cells at the crossroads of innate and adaptive immunity against infectious diseases at the mucosa. Mucosal Immunol. 2009; 2:403–411. [PubMed: 19587639]
53. Ivanov II, et al. Induction of intestinal Th17 cells by segmented filamentous bacteria. Cell. 2009; 139:485–498. [PubMed: 19836068]
54. Wu HJ, et al. Gut-residing segmented filamentous bacteria drive autoimmune arthritis via T helper 17 cells. Immunity. 32:815–827. [PubMed: 20620945]
55. Dewhirst FE, et al. Phylogeny of the defined murine microbiota: altered Schaedler flora. Appl Environ Microbiol. 1999; 65:3287–3292. [PubMed: 10427008]

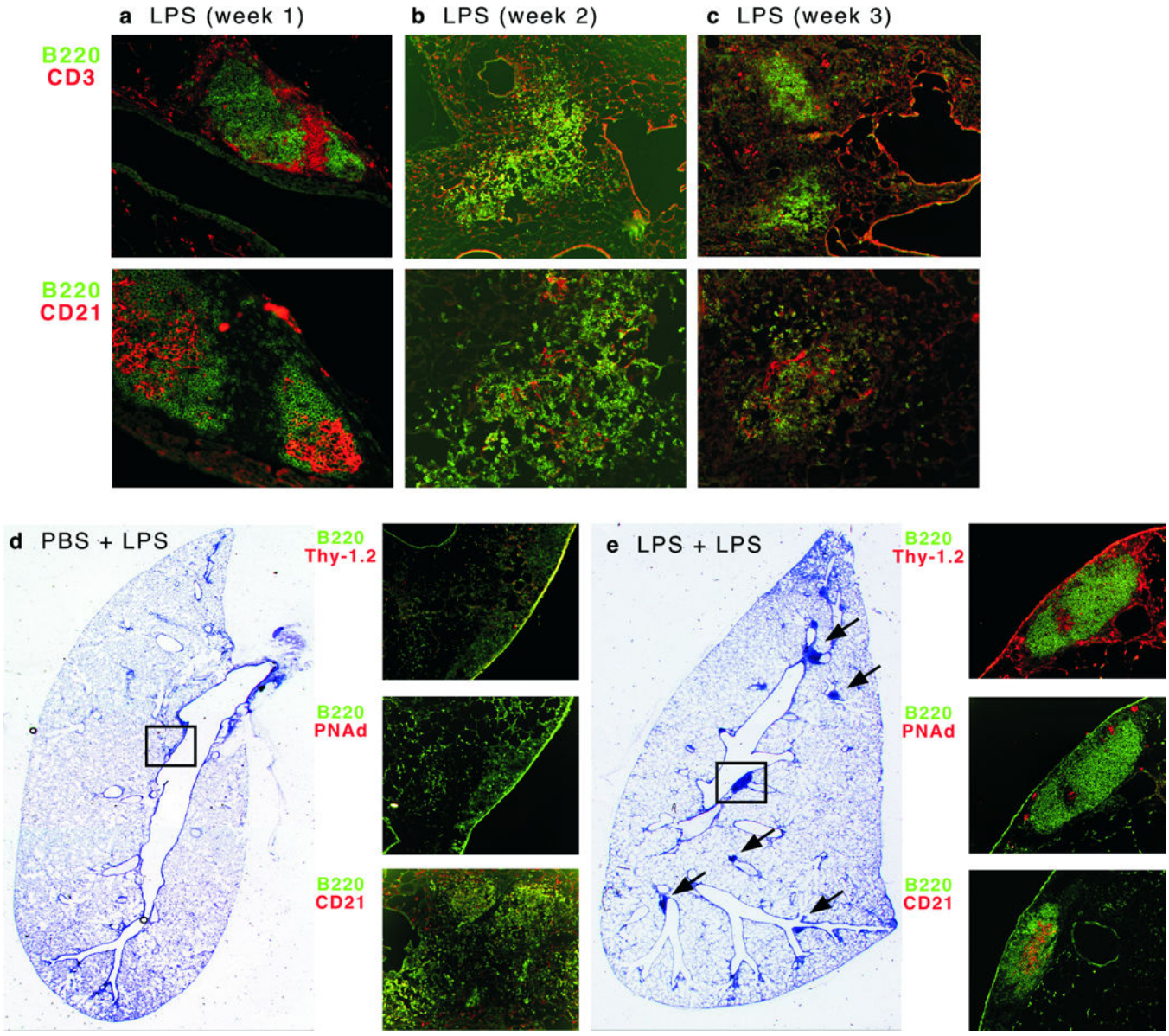

Fig. 1. Preferential development of iBALT in neonatal mice

(**a–c**) Mice were intranasally administered LPS starting on day 2 after birth (**a**), 2 weeks after birth (**b**) or 3 weeks after birth (**c**) and were subsequently infected with influenza when they were 8 weeks old. Lungs were obtained 3 weeks after infection and frozen sections were probed with antibodies against B220, CD3 and CD21. Images are representative of at least 3 independent experiments with 4–8 mice per group. (**d–e**) Neonatal mice were intranasally administered PBS (**d**) or LPS (**e**) and then intranasally administered LPS when they were 8 weeks old. Lungs were obtained 3 weeks after the last LPS administration and frozen sections were analyzed by histology (Diff-Quick) or probed with antibodies against B220, Thy-1.2, PNAd or CD21. The boxes in histology panels indicate the areas analyzed by fluorescent microscopy in serial sections. Arrows indicate areas of iBALT. Images are representative of 2 experiments with 4–8 mice per group.

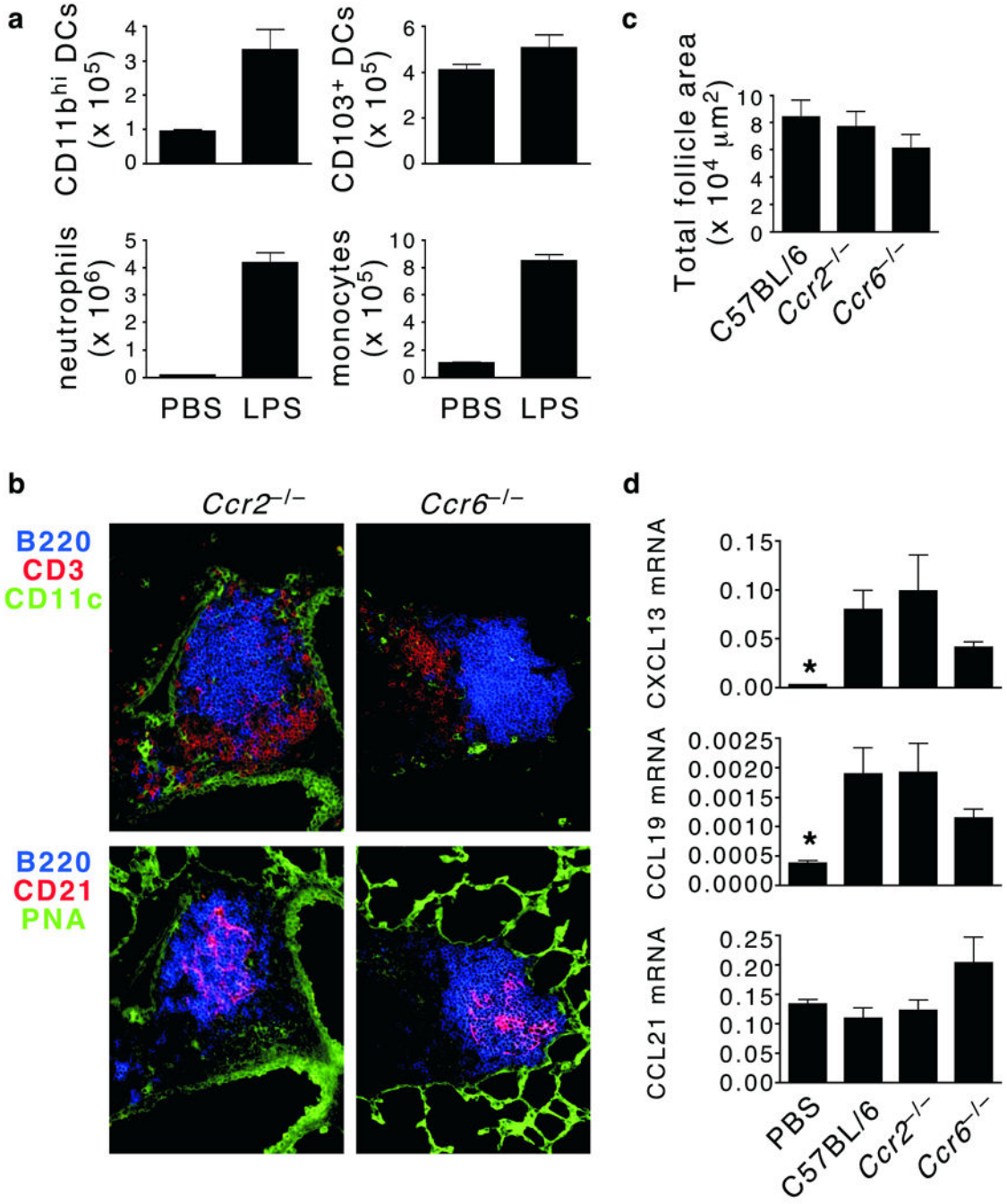

Fig. 2. iBALT forms independently of CCR2 and CCR6

(**a**) Neonatal C57BL/6 mice were intranasally administered either PBS or LPS. Lungs were collected 6 h after the last LPS administration and single cell suspensions were analyzed by flow cytometry for $B220^{-}CD11c^{+}MHCII^{+}CD11b^{hi}CD103^{-}$ DCs, $B220^{-}CD11c^{+}MHCII^{+}CD11b^{lo}CD103^{+}$ DCs, $CD11b^{+}7/4^{+}Ly6C^{+}Ly6G^{+}$ neutrophils and $CD11b^{+}7/4^{+}Ly6C^{+}Ly6G^{-}$ monocytes. Data are representative of 3 experiments with 4–8 mice per group. (**b**) Neonatal C57BL/6, *Ccr2*$^{-/-}$ and *Ccr6*$^{-/-}$ mice were intranasally administered LPS. Lungs were obtained 1 week after the last LPS administration and frozen

sections were probed with antibodies against B220, CD3 and CD21. Images are representative of 3 independent experiments with 3–5 mice per group. (**c**) The area of the lymphoid cell follicles in the lungs of mice of each genotype was determined using the outline tool in the Zeiss Axiovision software. Data are representative of 3 experiments with 3–5 mice per group and at least 1 slide per animal. Data are shown as mean ± standard deviation. (**d**) Neonatal mice were intranasally treated with LPS or PBS and total RNA was obtained from the lungs 6 h following the last LPS administration. RNA expression was analyzed by quantitative PCR for the indicated mRNAs and all values were normalized to GAPDH. These experiments were performed twice with 4–8 mice per litter. Data are shown as mean ± standard deviation.

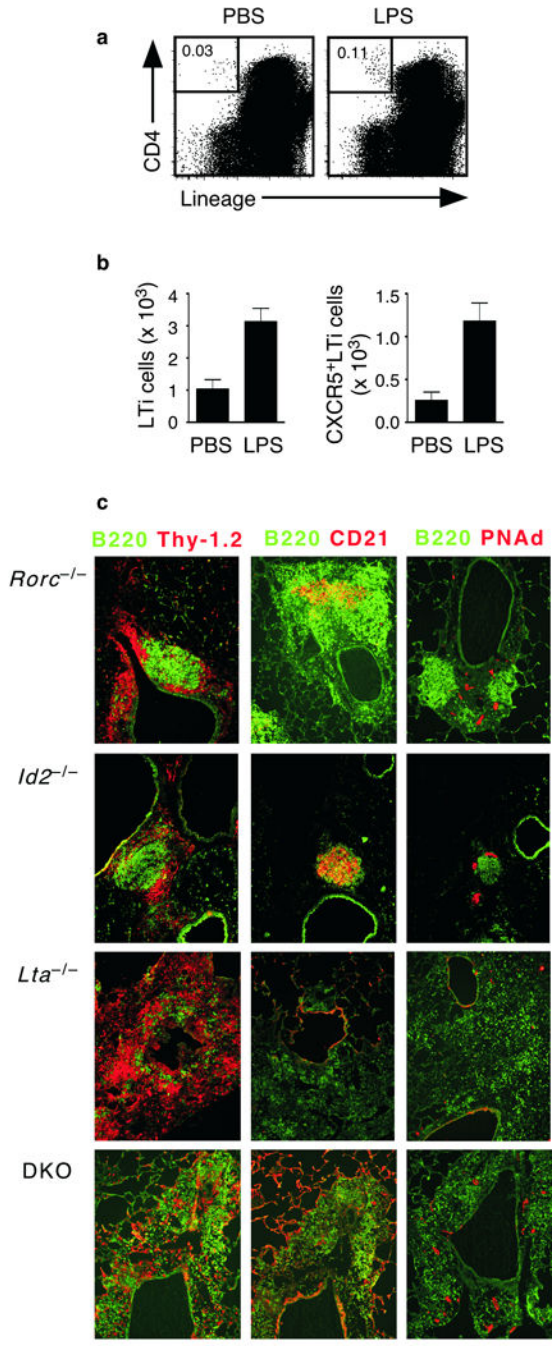

Fig. 3. LTi cells are not required for iBALT development

(**a**) Neonatal mice were intranasally administered either PBS or LPS and single cell suspensions from lungs were analyzed by flow cytometry 1 week after the last LPS administration. Lineage$^+$ cells were identified using a cocktail of antibodies against CD3, CD8, CD11b, CD11c, CD19, B220, NK1.1 and GR-1. The percentage of CD4$^+$lineage$^-$ cells is indicated in the boxes. (**b**) CD4$^+$lineage$^-$ LTi cells as well as CD4$^+$CXCR5$^+$lineage$^-$ LTi cells were enumerated. The data in **a** and **b** are representative of 2 independent experiments with 4–8 mice per group. Dare are shown as mean ± standard deviation. (**c**)

Neonatal mice were intranasally administered LPS and were subsequently infected with influenza when they were 8 weeks old. Lungs were obtained 3 weeks after infection and frozen sections were probed with antibodies against B220, Thy1.2, CD21 and PNAd. The images shown are representative of 4 experiments with 4–8 mice per group.

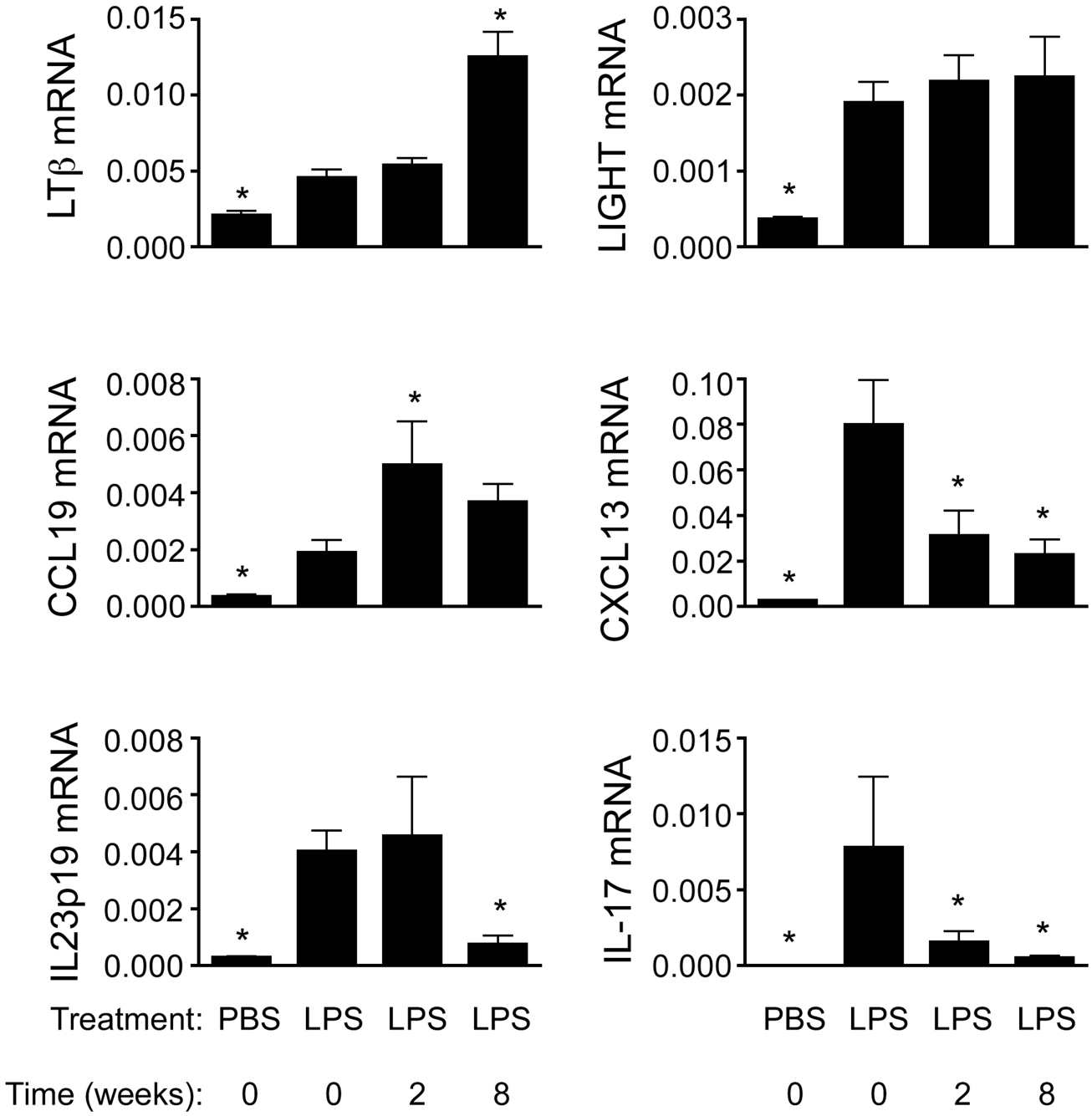

Fig. 4. Elevated expression of IL-17 in the lungs of LPS-treated neonates

Mice were intranasally administered 10 μg LPS 5 times (once every other day) starting on day 2, day 14 or 8 weeks after birth. Lungs were obtained 6 hours following the last LPS inoculation and total RNA was extracted. RNA expression was analyzed by quantitative PCR for the indicated mRNAs and all values were normalized to the expression of GAPDH. This experiment was performed 3 times with 4–8 mice per litter. Data are shown as mean ± standard deviation. Asterix indicate a significant difference ($p<0.05$ unpaired t test) from mice treated with LPS at 0 weeks.

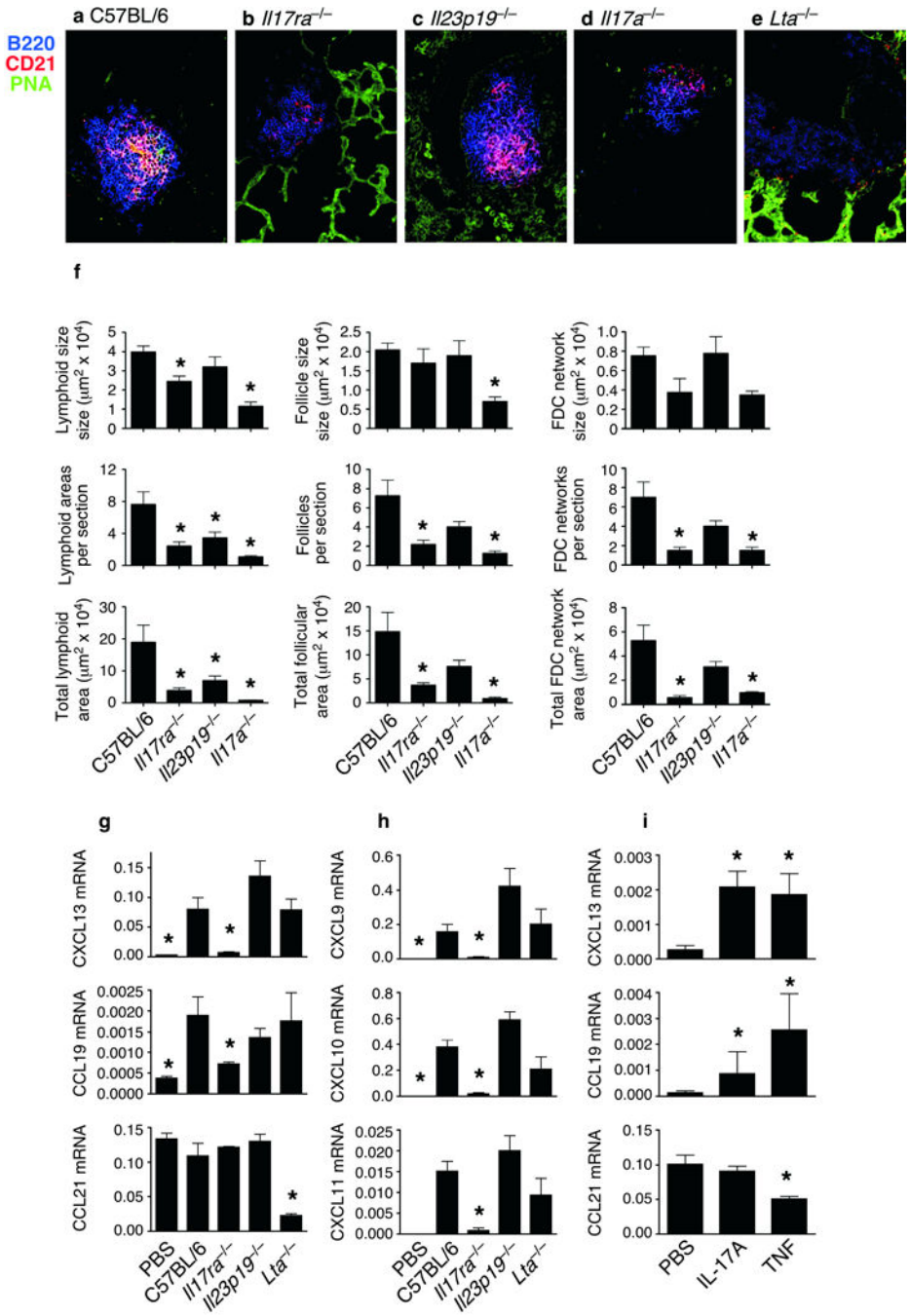

Fig. 5. IL-17 is required for the development of iBALT

(**a–e**) Neonatal mice were intranasally administered LPS and lungs were obtained 1 week following the last LPS administration and probed with antibodies against B220 and CD21. Images are representative of at least three mice per group. (**f**) The area of the lymphoid clusters, $B220^+$ B cell follicles or $CD21^+$ FDC networks was determined using the outline tool in the Zeiss Axiovision software. Data are shown as mean ± standard deviation from multiple slides of at least 3 mice per group. Asterix indicate a significant difference ($p<0.05$ unpaired t test) from C57BL/6 mice. (**g,h**) Neonatal mice were intranasally administered

LPS and lungs were obtained 6 hours following the last intranasal LPS administration and total RNA was extracted. RNA expression was analyzed by quantitative PCR for the indicated mRNAs and all values were normalized to GAPDH. Graphs indicate mean ± standard deviation. Asterix indicate a significant difference ($p<0.05$ unpaired t test) from C57BL/6 mice. These experiments were performed 2 times with 4–8 mice per litter. (**i**). Pulmonary fibroblasts were obtained from untreated neonatal lungs, stimulated with IL-17A or TNF and chemokine expression was measured by quantitative PCR. All values were normalized to GAPDH. Graphs indicate mean ± standard deviation. Asterix indicate a significant difference ($p<0.05$ unpaired t test) from C57BL/6 mice. This experiment was performed 3 times with similar results.

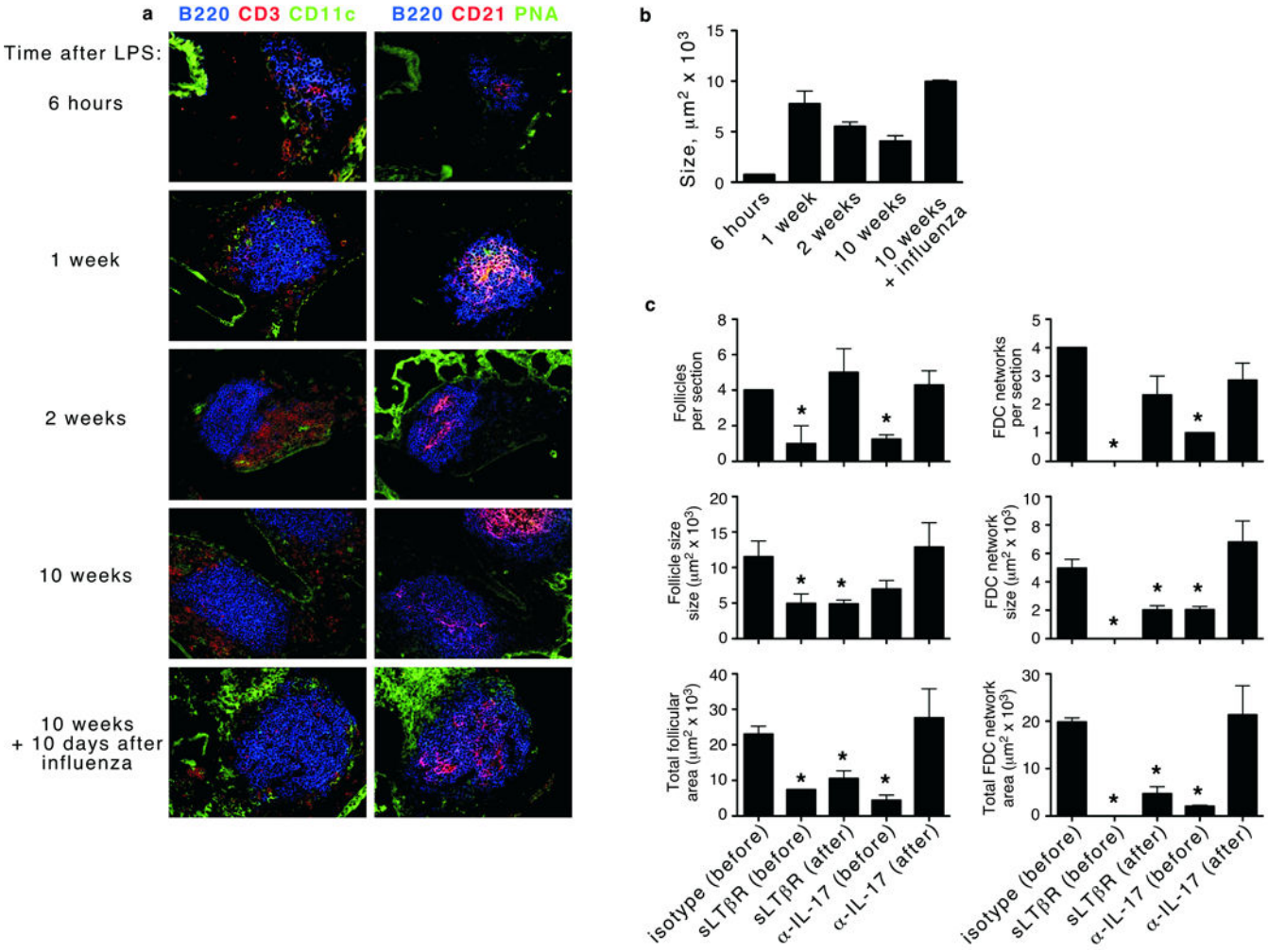

Fig. 6. IL-17 acts early in iBALT formation, but does not maintain its structure

(**a**) Neonatal mice were intranasally administered LPS and lungs were obtained at the indicated times and frozen sections were probed with antibodies against B220, CD3 and CD21. Images are representative of mice from 3 litters. (**b**) The total area of the CD21-CD35^{+} FDC networks in B cell follicles at each time was determined using the outline tool in the Zeiss Axiovision software. Bars represent mean ± standard deviation. This experiment was performed with at least 3 litters of mice with 4–8 mice per litter. (**c**) LPS was intranasally administered to neonatal mice and sLTβR-Ig or anti-IL-17 blocking reagents were intranasally administered either 1 day before the last LPS administration or 1 week after the last LPS administration. Lungs were obtained for histology 1 week following treatment. B cell clusters or FDC networks were enumerated by immunofluorescence microscopy. The area of individual B cell clusters or CD21^{+} FDC networks was determined using the outline tool in the Zeiss Axiovision software. Bars represent mean ± standard deviation obtained from multiple slides from at least 3 mice per group. Asterix indicate a significant difference ($p<0.05$ unpaired t test) from C57BL/6 mice.

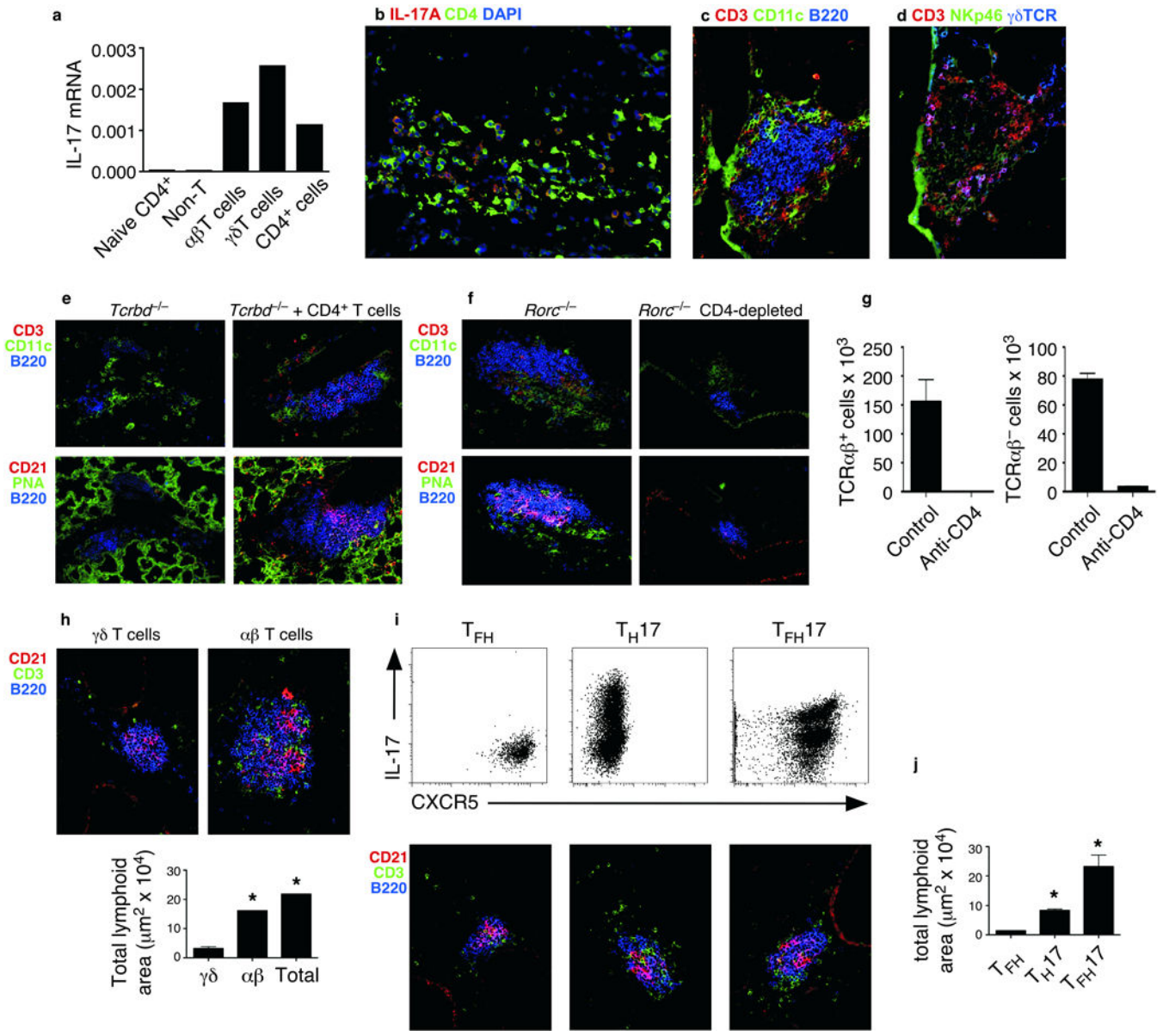

Fig. 7. IL-17-producing T cells promote iBALT formation

(**a**) IL-17 expression was measured by quantitative PCR in αβT cells, γδT cells and CD4$^+$ cells from lungs of LPS-treated neonates and in CD4$^+$ cells from naïve LNs. Data are representative of 2 experiments from 5–10 pooled mice. (**b–d**) Frozen sections from LPS-treated neonatal lungs were probed with antibodies to IL-17A and CD4 (**b**) or with antibodies to CD3, CD11c, B220, NKp46 and γδTCR (**c–d**). Serial sections are shown. Images are representative of 2 experiments with 4–8 mice per litter. (**e**) Neonatal *Tcrbd*$^{-/-}$ mice received no cells or CD4$^+$ T cells and were intranasally administered LPS. Lungs were obtained 1 week following the last LPS administration and frozen sections were probed with antibodies to CD3, CD11c, B220, CD21 and PNA. (**f–g**) *Rorc*$^{-/-}$ mice were depleted with anti-CD4 or isotype control one day before the last LPS administration. Lungs were obtained 1 week later and probed with antibodies to CD3, CD11c, B220, CD21 and PNA (**f**).

Depletion of $CD4^+$ αβT cells and γδT cells was confirmed using flow cytometry (**g**). Bars indicate mean ± standard deviation. These experiments were performed twice with 4–8 mice per litter. (**h**) γδT cells or αβT cells were adoptively transferred to neonatal, LPS-treated *Tcrbd*$^{-/-}$ recipients. Lungs were obtained 1 week after the last LPS administration and frozen sections were probed with antibodies against CD21, CD3 and B220. Morphometric analysis of lymphoid areas was performed. Images are representative of 2 independent experiments with 4–8 mice per group. Graphs show the mean ± standard deviation of multiple slides from 4–8 mice per group. (**i,j**) OVA-specific T_{FH}, Th17 and $T_{FH}17$ cells were transferred to neonatal *Tcrbd*$^{-/-}$ recipients, which were challenged with LPS and OVA and analyzed by immunofluorescence for CD21, CD3 and B220 1 week after the last OVA administration. Flow cytometry plots represent IL-17 and CXCR5 expression on cells prior to transfer. (**j**) The total area of B cell follicles was determined. Bars represent mean ± standard deviation. Asterix indicate a significant difference ($p<0.05$ unpaired t test) from the T_{FH} group. FACS plots, images and graphs represent 1 of 2 experiments with 3–7 mice per group.